Soils and Foundations 2014;54(3):502–514

The Japanese Geotechnical Society

Soils and Foundations

www.sciencedirect.com
journal homepage: www.elsevier.com/locate/sandf

Numerical method for evaluating the lateral resistance of sleepers in ballasted tracks

Yohei Koike[a], Takahisa Nakamura[b], Kimitoshi Hayano[c,*], Yoshitsugu Momoya[b]

[a]Graduate School of Urban Innovation, Yokohama National University, 79-5 Tokiwadai, Hodogaya-ku, Yokohama, Kanagawa 240-8501, Japan
[b]Track Structures and Geotechnology Laboratory, Railway Technical Research Institute, 2-8-38 Hikari-cho, Kokubunji, Tokyo 185-8540, Japan
[c]Faculty of Urban Innovation, Yokohama National University, 79-5 Tokiwadai, Hodogaya-ku, Yokohama, Kanagawa 240-8501, Japan

Received 28 July 2013; received in revised form 24 December 2013; accepted 30 January 2014
Available online 29 April 2014

Abstract

Ballasted track sleepers have the important function of providing sufficient lateral resistance to prevent the lateral movement of rails. If the lateral force induced by the thermal expansion of steel rails overcomes the lateral resistance of sleepers, rail buckling may occur. More attention has been paid to this problem of lateral stability since the introduction of continuous welded rails. However, there is a high degree of uncertainty in the prediction of the lateral resistance of sleepers. In view of the foregoing, a series of laboratory tests was conducted on 1/5-scale models to evaluate the lateral resistance of sleepers. Single-sleeper pullout tests and track panel pullout tests were conducted on different types of concrete sleepers. The results of the pullout tests revealed the effects of the sleeper shape, the sleeper spacing, and the number of sleepers on the lateral resistance. Based on the model test results, a new numerical method for evaluating the lateral resistance of sleepers is proposed.

Keywords: Ballasted track; Lateral resistance; Sleeper shape; Piled group effect; Track panel pullout test

1. Introduction

Railway sleepers are small shallow foundations whose primary function is to support rails and traffic loads. However, under repeated traffic loading, sleepers may gradually settle, especially in the case of ballasted tracks. This is due to the plastic compression of the ballast and the underlying subgrade. Excessive settlement of the sleepers increases the possibility of railway accidents and reduces the comfort of rail rides. Therefore, efforts have been made to investigate the deformation characteristics of ballasted tracks (e.g., Ishikawa and Namura, 1995; Dahlberg, 2001; Namura et al., 2005; Momoya et al., 2005; Indraratna, 2011).

Another important function of sleepers on ballasted tracks is to provide sufficient lateral resistance to prevent the lateral movement of the rails. A significant increase in the temperature of steel rails may produce thermal elongation. The thermal elongation of steel rails induces excessive axial forces; this creates a tendency for the steel rails to bend and to exert a lateral force on the sleepers. If the lateral force overcomes the lateral resistance of the sleepers, rail buckling may occur, as shown in Fig. 1. More attention has been paid to this issue since the introduction of continuous welded rails (CWR) (e.g., Kerr, 2004; Xavier, 2012). CWR are long rails that allow for

*Corresponding author. Tel.: +81 45 339 4037.
E-mail address: hayano@ynu.ac.jp (K. Hayano).
Peer review under responsibility of The Japanese Geotechnical Society.

Production and hosting by Elsevier

http://dx.doi.org/10.1016/j.sandf.2014.04.014
0038-0806/

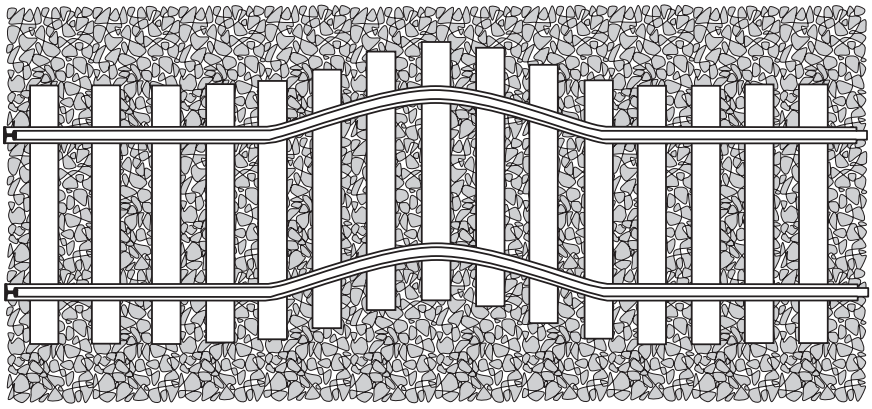

Fig. 1. Schematic view of lateral instability of ballasted tracks.

higher travel speeds and ensure more comfortable rides by reducing the number of joints. However, their length makes the investigation of buckling resistance even more important.

So far, several studies have been conducted to evaluate the buckling strength of CWR in ballasted tracks. Most of them were numerical studies. Asanuma et al. (2012) conducted elasto-plastic and finite displacement analyses to investigate the buckling temperature. They concluded that the lateral resistance of sleepers and initial track misalignments and track curvatures had significant effects on the minimum buckling resistance strength of CWR. Arbabi and Khalighi (2011) used Mathcad to conduct a parametric study of the combined effects of temperature and earthquakes on the lateral stability of tracks. They noted that the lateral instability of tracks can be induced by earthquakes because shaking ballasts significantly reduce the lateral resistance of sleepers. Bao and Barenberg (1997) conducted 3D stability analyses to investigate the effects of temperature and mechanical loads on the lateral instability of tracks. They emphasized the reduction in lateral resistance that occurs when the sleepers are lifted by the vertical loads of vehicles, as it significantly reduces track stability.

As mentioned above, the lateral resistance of sleepers is an important parameter in the evaluation of the lateral stability of ballasted tracks, irrespective of the analytical method. The method chosen to evaluate the maximum lateral resistance and the modeling of the displacement–load curve significantly affects the analytical results. Pullout tests are usually used to estimate the lateral resistance of full-scale sleepers in situ or by experiments. As noted by Le Pen and Powrie (2012), pullout tests are generally one of the following two types:

(1) Single-sleeper pullout test: a sleeper is detached from the rails and pulled out by a machine attached to the rails, and the load/deflection response is recorded.
(2) Track panel pullout test: a section of the track is pulled sideways from the rail head. The test section may be isolated (cut) or attached to the rest of the line (uncut).

For example, Le Pen and Powrie (2012) conducted full-scale model tests on a single concrete sleeper to determine the applicability of their proposed equilibrium calculations. They investigated the effects of the bottom resistance, the side resistance, and the end resistance of the sleepers on the total lateral resistance by changing parts of the ballast beside the sleeper. It was found that, out of the total for each component, 26–35% was for the base, 37–50% was for the side, and 15–37% was for the end. These values are different from those reported in Lichtberger (2007), which suggested 45–50% for the base, 10–15% for the side, and 35–40% for the end. These facts indicate that the situation is more complex than the conventionally assumed equal split, which is only approximately correct in certain circumstances.

On the other hand, Takatani et al. (1987) conducted full-scale model tests on a track panel with six sleepers. The sleepers were equally displaced in a rigid frame. The conclusions drawn from the test results were similar to those of Le Pen and Powrie (2012). In addition, they investigated the effects of the number of sleepers in the track panel pullout tests on the lateral resistance. It was found that the lateral resistance per sleeper of a track panel with two sleepers was higher than that of a track panel with six sleepers. The reason for this, however, was not identified. Moreover, Kabo (2006) reported that the levels of lateral resistance obtained from single-sleeper pullout tests were generally higher than those obtained from track panel pullout tests. He also noted that the boundary conditions of both tests differed from those in real life.

It can be seen, therefore, that several aspects must be considered in order to precisely evaluate the lateral resistance of the sleepers of ballasted tracks. First, there is a high degree of uncertainty when predicting the lateral resistance of a single sleeper. This is not only because of the complicated material properties of the ballast, but also because of the uncertain effects of the bottom, the side, and the end resistance of sleepers of various shapes. The effect of sleeper spacing on the lateral resistance is also not clear. The differences between the results of single-sleeper pullout tests and track panel pullout tests may be due to the effects of sleeper spacing, although the mechanisms have yet to be studied in detail. Finally, the effects of the boundary conditions of track panel pullout tests on the lateral resistance per sleeper have not been properly clarified. Increasing the number of sleepers in a longer track panel may reduce the effects of the free ends. However, pullout tests are

usually conducted on short panels with two to five sleepers due to the limited loading capacity of the machines.

Therefore, to investigate these aspects in detail, we conducted a series of laboratory tests on models whose sizes were 1/5 of the actual parts. Single-sleeper pullout tests and track panel pullout tests were conducted on several types of concrete sleepers. The effects of the sleeper shape, the sleeper spacing, and the number of sleepers on the lateral resistance during the pullout tests were investigated. The test results and the experimental procedures are presented in this paper. In addition, the results of the tests are used to propose a new method for evaluating the lateral resistance of sleepers.

2. Sleepers, model test apparatus, and test conditions

In this research, tests were conducted on 1/5-scale track models. Therefore, we prepared 1/5-scale models of sleepers and ballast. Kusuda et al. (2012) found that 1/5-scale model tests produced levels of lateral resistance that were approximately 1/125 of those produced by full-scale tests. The observation was explained as follows.

The lateral resistance of a sleeper is composed of its bottom, its side, and its end resistance. As the sleeper is scaled down by five, the area of its bottom is 1/25 of that of a full-scale sleeper, and the overburden pressure at the bottom of the sleeper, induced by its weight, is 1/5 of that of a full-scale sleeper. Therefore, the friction between the bottom of the sleeper and the ballast, which is the bottom resistance, becomes 1/125 of that of actual sleepers. It can be assumed, however, that the end resistance is induced by the passive earth pressure of the ballast, so that it primarily depends on the shear strength of the ballast. Since the sleeper depth is 1/5 of that of a full-scale sleeper, the confining pressure of the ballast may be 1/5 of that of actual ballast, resulting in a shear strength that is 1/5 of that of real ballast. Considering that the area at the end of the sleeper is 1/25 of that of a full-scale one, the end resistance is fractioned by 125. Similarly, the side resistance is 1/125 of that of an actual sleeper.

The above was observed in this study, and therefore, we did not compare full-scale test results with the results obtained for the 1/5-scale model. A detailed description of the preparation for the model tests is given in the following sections.

2.1. Sleepers

The six types of sleepers shown in Fig. 2 were prepared for the model tests. The sizes of all the sleepers were 1/5 of those of real ones. Although sleepers on real tracks are designed to be pre-stressed concrete, the sleepers which were prepared for

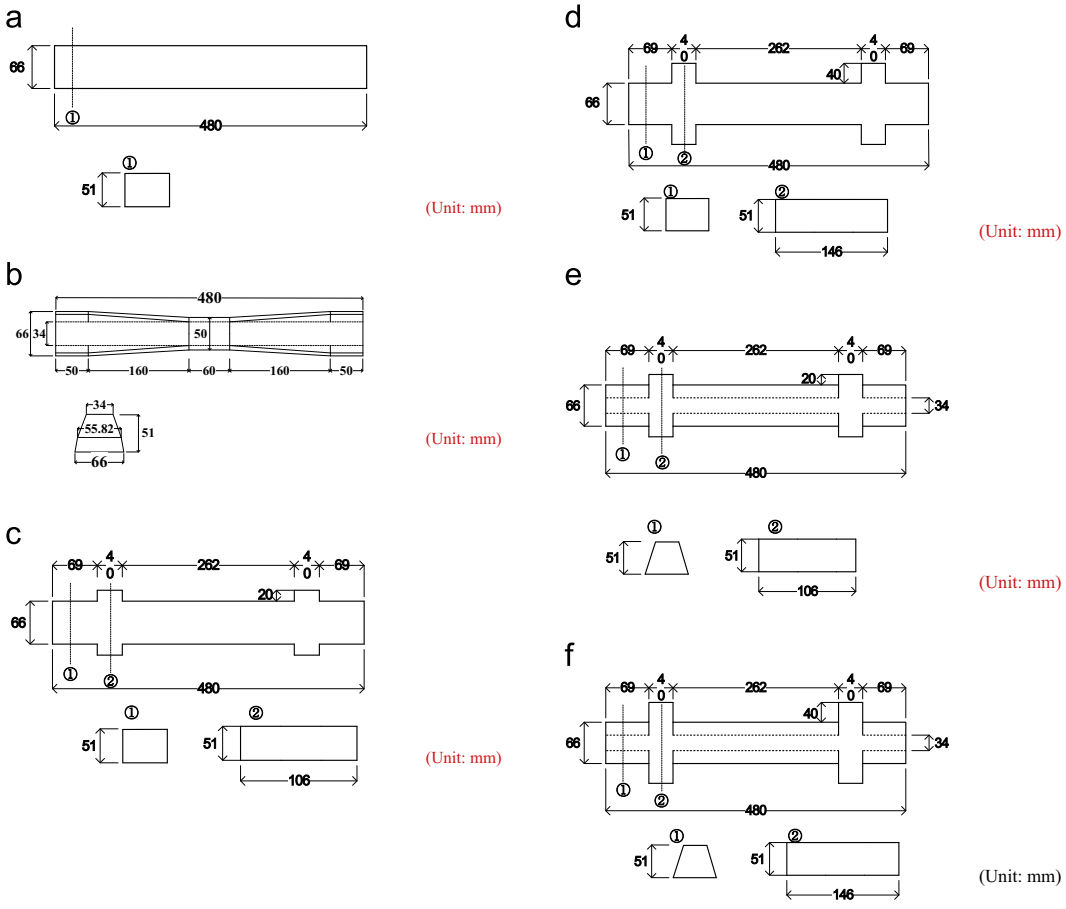

Fig. 2. Sleepers prepared for model tests. (a) Rectangular parallelepiped sleeper, (b) 3H sleeper, (c) 20-mm-winged sleeper with rectangular ends, (d) 40-mm-winged sleeper with rectangular ends, (e) 20-mm-winged sleeper with trapezoidal ends and (f) 40-mm-winged sleeper with trapezoidal ends.

the model tests here were made from mortar and not pre-stressed. The sleeper specifications are as follows:

(a) Rectangular parallelepiped sleeper (see Fig. 2(a))

The sleeper had a rectangular parallelepiped shape and was 480 mm long, 66 mm wide, and 51 mm high. Its total volume was 1616 cm^3. Five rectangular parallelepiped sleepers were prepared for the model tests. The average density of the sleepers was 2.33 g/cm^3. The parallelepiped sleepers were used in the experiments for a comparison with the other types of sleepers.

(b) 3H sleeper (see Fig. 2(b))

The shape of the 3H sleeper was similar to that of the rectangular parallelepiped sleeper. However, the cross section was not rectangular, but had the shape of two combined trapezoids. As shown in the figure, the top and the bottom of the cross section at both ends of the sleeper were 34 mm and 66 mm wide, respectively. The bottom width gradually decreased to 50 mm at the middle from both ends. The height of the ends of the sleeper was 51 mm and it had a volume of 1032 cm^3. Five 3H sleepers with an average density of 2.32 g/cm^3 were prepared for the model tests. The 3H sleeper is often used in high-speed railway (Shinkansen) tracks.

(c) and (d) Winged sleepers with rectangular ends (see Fig. 2(c) and (d))

The winged sleepers had four wing-like projections added to the bilateral sides of the rectangular parallelepiped sleeper. The projections were either 20 mm or 40 mm long, as shown in Fig. 2(c) and (d), respectively. As noted by Zakeri et al. (2012), the wings are expected to increase the lateral resistance. The cross sections at both ends of the sleepers were 66 mm by 51 mm rectangles. However, the cross sections of the 20-mm-long wings were 106 mm by 51 mm rectangles, whereas those of the 40-mm-long wings were 146 mm by 51 mm rectangles. The volume of the sleeper with 20-mm wings was 1779 cm^3, whereas that of the sleeper with 40-mm wings was 1942 cm^3. Five 20-mm-winged sleepers with an average density of 2.32 g/cm^3 were prepared for the model tests, whereas only one 40-mm-winged sleeper with a density of 2.29 g/cm^3 was prepared for the model tests.

(e) and (f) Winged sleepers with trapezoidal ends (see Fig. 2(e) and (f))

The shapes of these sleepers were very similar to those of the winged sleepers with rectangular ends. However, the cross section at their ends was not rectangular, but trapezoidal, as shown in Fig. 2(e) and (f). The top and the bottom widths were 34 and 66 mm, respectively. The cross sections of the wings were the same as those of the winged sleepers with rectangular ends. The volume of the 20-mm-winged sleeper was 1453 cm^3 and that of the 40-mm-winged sleeper was 1616 cm^3. Five 20-mm-winged sleepers with an average density of 2.33 g/cm^3 were prepared for the model tests. However, only one 40-mm-winged sleeper with a density of 2.30 g/cm^3 was prepared for the model tests.

2.2. Ballast

To prepare the 1/5-scale ballasted tracks, ballast particles that were 1/5 of the actual ones were used. The ballast was made from crushed Andesite stones obtained from Yamanashi Prefecture in Japan. The particles had angular shapes, as shown in Fig. 3(a). The particle size distribution curve is shown in Fig. 3(b). The range in particle size distribution specified in the Japanese railway technical standard is also shown in the figure. Maximum particle size D_{max} is 11.2 mm, average particle size D_{50} is 7.6 mm, and uniformity coefficient U_c is 1.57.

2.3. Model test apparatus and test conditions

The model test apparatus shown in Fig. 4 was used to load the sleepers horizontally. The model test apparatus consisted of a sand box and a horizontal loading jack. The load cell had a maximum capacity 1.96 kN. The sand box was 1245 mm long, 970 mm wide, and 150 mm high. It was mainly made of aluminum. As can be seen from the figure, sandpaper was attached to the bottom plate to ensure frictional resistance between the ballast and the bottom plate.

In preparing the ballasted tracks, the track beds were first constructed using the ballast in the sand box. A single sleeper

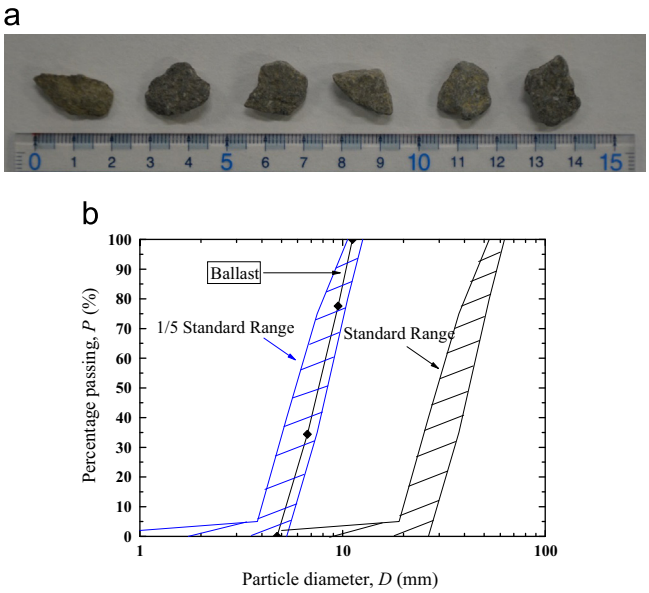

Fig. 3. Ballast used for model tests and its particle size distribution curve. (a) Ballast (crushed stones) and (b) Particle size distribution curve of ballast.

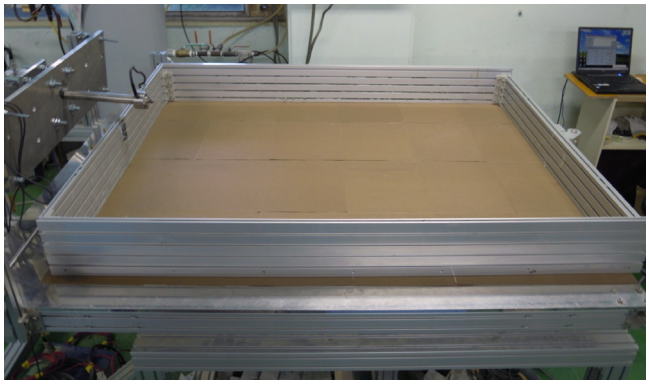

Fig. 4. Model test apparatus for horizontal loading of sleepers.

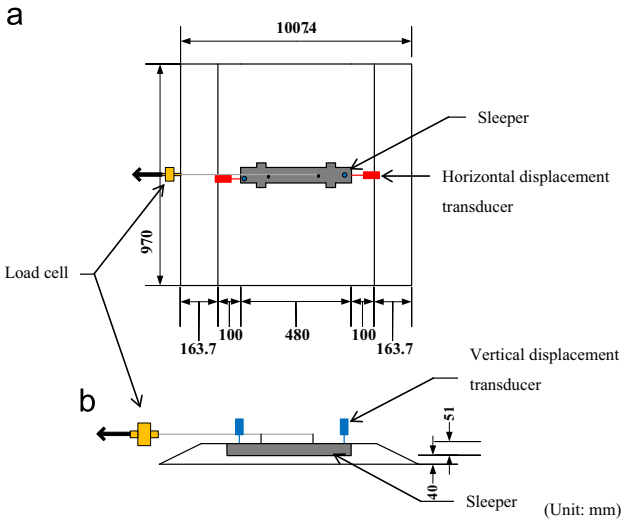

Fig. 5. Schematic views of ballasted tracks for single-sleeper pullout tests conducted on 20-mm-winged sleeper. (a) Top view and (b) side view.

or track panel (consisting of several sleepers and a rigid frame) was then set in the ballast. The horizontal loading jack was used to pull out a single sleeper or track panel using a tie rod and a constant displacement rate. The lateral resistance of the single sleeper or the track panel was measured by the load cell, which was connected to the tie rod. Details of the construction of the ballasted tracks are given below.

2.3.1. Construction of ballasted tracks for single-sleeper pullout tests

Fig. 5 is a schematic of the ballasted tracks that were prepared for the single-sleeper pullout tests. First, the track bed was gradually constructed from ballast using the tamping and vibration methods to achieve a dry density of 1.60 g/cm^3. Zakeri and Sadeghi (2007) conducted pullout tests on a full-scale track with compacted ballast under accumulated traffic loadings and immediately after tamping. They observed that a reduction in the lateral resistance of the sleepers may occur immediately after tamping due to the loosening of the ballast. Maximum care was taken, therefore, to achieve a uniform distribution of the ballast density and to reproduce it in every test.

The track bed was rectangular and measured 1007 mm by 970 mm at the bottom, and 680 mm by 970 mm at the top. The total thickness of the track bed was 91 mm. During the construction of the track bed, a single sleeper was embedded in the ballast. Fig. 6 shows a typical 20-mm-winged sleeper embedded in the ballast.

After construction of the ballasted track, four displacement transducers were installed close to both ends of the single sleeper, as shown in Fig. 5, to measure the vertical and the horizontal displacements during horizontal loading. The displacement transducers were carefully set along the longitudinal axis of the sleeper so they would not be crossed by the tie-rod. In addition, a digital camera was set about 1200 mm above the sleeper to capture digital images of the ballast and the sleeper

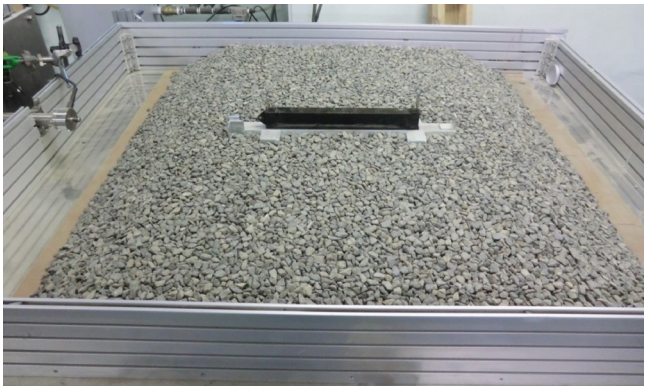

Fig. 6. 20-mm-winged sleeper embedded in ballast.

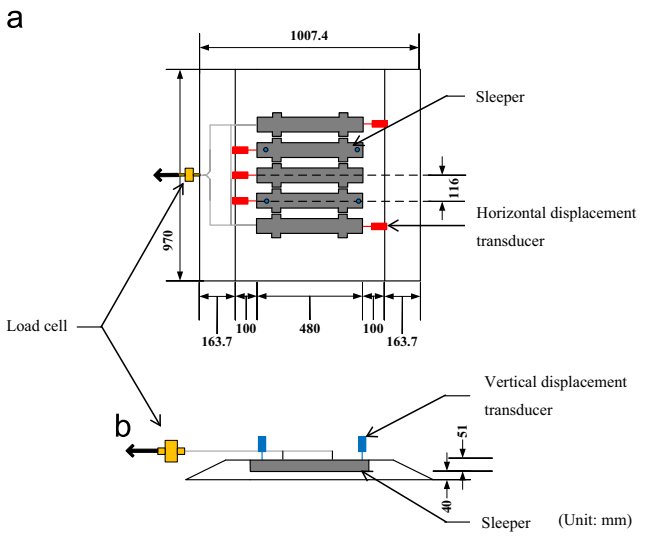

Fig. 7. Schematic views of ballasted tracks for track panel pullout tests using five 20-mm-winged sleepers. (a) Top view and (b) side view.

during loading. The digital camera had a resolution of 16 million pixels. The single-sleeper pullout test was conducted six times to investigate the lateral resistance of the different types of sleepers mentioned in Section 2.1.

2.3.2. Construction of ballasted tracks for track panel pullout tests

Fig. 7 is a schematic of the ballasted tracks prepared for the track panel pullout tests. The track bed preparation procedure was the same as that for the single-sleeper pullout tests. However, three, five, or seven sleepers were embedded in the ballast. The sleepers were spaced at 116 mm, as shown in the figure. A rigid frame was set on the embedded sleepers to connect them. The weight of the rigid frame was 1/125 of that of actual rails. Fig. 8 shows the rigid frame and five rectangular parallelepiped sleepers embedded in the ballast.

After construction of the ballasted track, five displacement transducers were set at the prescribed positions shown in Fig. 7 to measure the horizontal displacements of the sleepers. Four displacement transducers were also set at predetermined positions to measure the vertical displacements of the sleepers.

Fig. 8. Rigid frame and five rectangular parallelepiped sleepers embedded in roadbeds.

The track panel pullout tests with five sleepers were conducted using the rectangular parallelepiped sleepers, the 3H sleepers, the 20-mm-winged sleepers with rectangular ends, and the 20-mm-winged sleepers with trapezoidal ends. On the other hand, the track panel pullout tests with three or seven sleepers were conducted using the 3H sleepers and the 20-mm-winged sleepers with trapezoidal ends.

2.4. Horizontal loading

Horizontal loading was conducted at a constant displacement rate of 0.4 mm/min in both the single-sleeper pullout tests and the track panel pullout tests. The lateral resistance and the vertical and the horizontal displacements of the sleepers were continuously recorded using a data logger until the horizontal displacements exceeded 10 mm.

3. Effects of sleeper weight and shape on lateral resistance

3.1. Lateral resistance for single-sleeper pullout tests

The relationship between the horizontal load and the horizontal displacement of the sleepers, obtained from the single-sleeper pullout tests, is shown in Fig. 9(a). As can be seen from the figure, the horizontal load of all the sleepers gradually increased with an increasing horizontal displacement until the horizontal load reached a maximum. Beyond the maximum horizontal load, the horizontal load of most of the sleepers was almost constant with an increasing horizontal displacement.

The relationship between the vertical displacement and the horizontal displacement of the sleepers, obtained from the single-sleeper pullout tests, is shown in Fig. 9(b). Here, positive values for the vertical displacement indicate the upward movement of the sleepers. In the figure, the solid lines represent the vertical displacement measured at the sleeper end far from the loading jack (back side), whereas the dotted lines represent the vertical displacement measured at the sleeper end close to the loading jack (front side). The vertical displacement on the back side of the 3 H sleeper and that on the front side of the rectangular parallelepiped sleeper could not be measured owing to errors in setting the positions

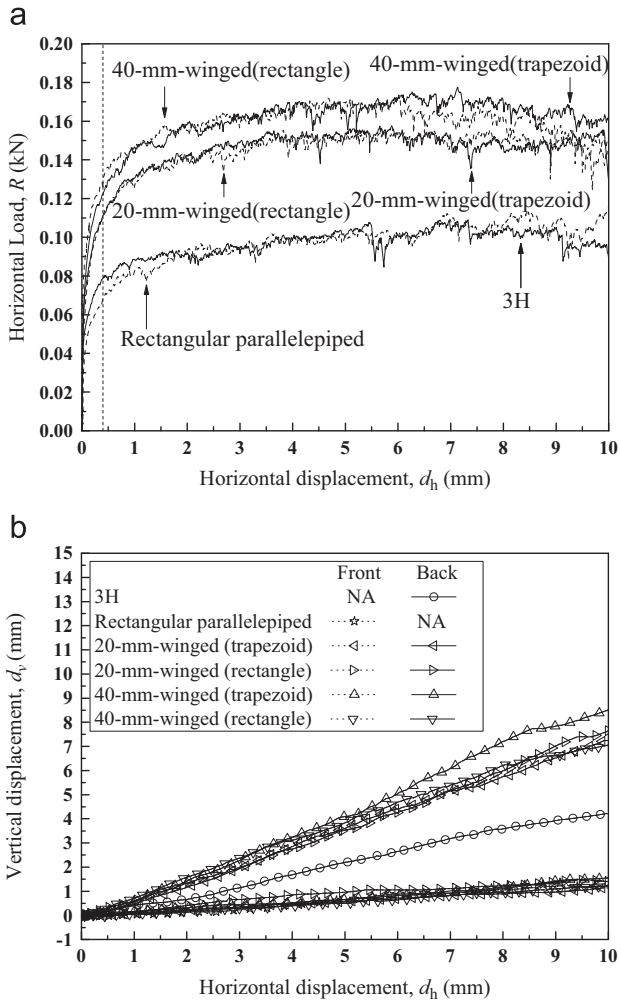

Fig. 9. Horizontal loads, vertical displacements, and horizontal displacements obtained from single-sleeper pullout tests. (a) Relationship between horizontal load and horizontal displacement and (b) relationship between vertical displacement and horizontal displacement.

of the displacement transducers. It can be seen from the figure that the sleepers moved upward. This indicates the positive dilatancy of the ballast; it was induced by shearing close to the bottom of the sleeper. It can also be seen from the figure that the vertical displacements on the front side were significantly smaller than those on the back side. This indicates a rotation of the sleeper by the moment that was generated during horizontal loading.

A detailed consideration of the results in Fig. 9(a) shows that the relationship between the horizontal load and the horizontal displacement for the 20-mm-winged sleeper with rectangular ends is very similar to that of the 20-mm-winged sleeper with trapezoidal ends. Similarly, the corresponding relationship for the 40-mm-winged sleeper with rectangular ends is very similar to that of the 40-mm-winged sleeper with trapezoidal ends. It can also be seen from the figure that the same relationship for the rectangular parallelepiped sleeper is similar to that for the 3H sleeper.

From the above observations, a question arises about the sleeper shapes that significantly affect the lateral resistance.

Apparently, the difference between the cross section shapes of the winged sleepers had little effect on the lateral resistance, whereas the widths of their wings did seem to have a significant effect. These issues will be discussed in detail in the following sections.

3.2. Effects of sleeper weight

According to Kabo (2006), the lateral resistance obtained from single-sleeper pullout tests is generally higher than that obtained from track panel pullout tests. To resolve this difference, RTRI (2012) suggested that the lateral resistance obtained at a horizontal displacement of 2.0 mm in the single-sleeper pullout tests should be used to represent the lateral resistance for the track panel pullout tests. This can be simply expressed as follows:

$$R_{\text{panel}} \cong R_{\text{single}}^{2.0\ \text{mm}}(\text{in full scale}) \tag{1}$$

where R_{panel} denotes the lateral resistance in the track panel pullout tests and $R_{\text{single}}^{2.0\ \text{mm}}$ denotes the lateral resistance at a horizontal displacement of 2.0 mm in the single-sleeper pullout tests.

Considering the scale of the model tests, the lateral resistance of the sleepers at a horizontal displacement of 0.4 mm, $R_{\text{single}}^{0.4\ \text{mm}}$, in the model tests is equivalent to $R_{\text{single}}^{2.0\ \text{mm}}$ in the full-scale tests. This is because the levels of ballast strain mobilized in the model tests are similar to those in real tracks. Therefore, the following relationship can be suggested, which was also observed in previous studies (Nakamura et al., 2010; Kusuda et al., 2012).

$$R_{\text{panel}} \cong R_{\text{single}}^{0.4\ \text{mm}}(\text{in } 1/5-\text{scale}) \tag{2}$$

$R_{\text{single}}^{0.4\ \text{mm}}$ can be evaluated from the relationships shown in Fig. 9(a). The ratio of $R_{\text{single}}^{0.4\ \text{mm}}$ to $R_{\text{single}}^{10\ \text{mm}}$ ranged from 74% to 88%, with the exception of that for the rectangular parallelepiped sleeper, which was 59%. The average for all the sleepers was 77%. The obtained ratios are consistent with those reported in RTRI (2012).

Fig. 10 shows a graph of $R_{\text{single}}^{0.4\ \text{mm}}$ against the weight of the sleepers, W_{sleeper}. As can be seen from the figure, $R_{\text{single}}^{0.4\ \text{mm}}$ was not consistent with W_{sleeper}. For example, $R_{\text{single}}^{0.4\ \text{mm}}$ for the 40-mm-winged sleeper with trapezoidal ends was quite a bit higher than that for the rectangular parallelepiped sleeper, although W_{sleeper} was almost the same for the two types of sleepers. This suggests that side frictional resistance R_{side} and end resistance R_{end} (the earth pressure acting on the sleeper ends) significantly affected the lateral resistance of the sleepers.

3.3. Contributory effects of side frictional resistance and end resistance

Several studies have been conducted on the prediction of the lateral resistance of shallow foundations. Most of them required frictional resistance between the foundation and the ground. Similarly, for the estimation of the lateral resistance of conventional sleepers, such as the parallelepiped and the 3H

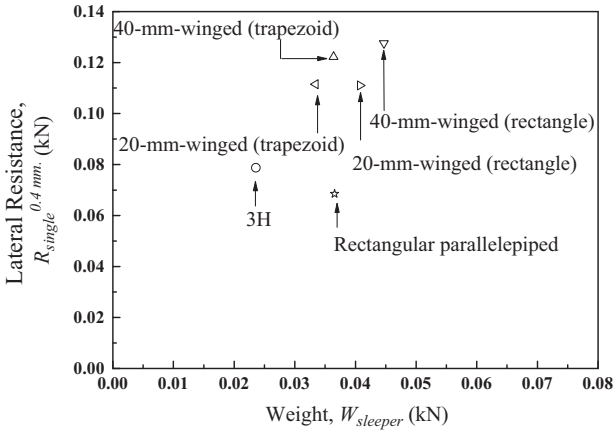

Fig. 10. Relationship between lateral resistance and weight obtained from single-sleeper loading tests.

sleepers, RTRI (2012) suggests the following equation:

$$R_{\text{total}} = aW_{\text{sleeper}} + b\gamma_{\text{ballast}}S_{\text{end}} + c\gamma_{\text{ballast}}S_{\text{side}} \tag{3}$$

where a, b, and c are the constant parameters that depend on the sleeper material. Here, S_{side} is the first moment on the side face of the sleepers with respect to the upper edge, and S_{end} is the first moment on the end face of the sleepers with respect to the upper edge. The first, second, and third terms on the right-hand side of Eq. (3) represent the contributory effect of bottom resistance R_{bottom}, end resistance R_{end}, and side resistance R_{side} of the sleeper, respectively.

Eq. (3) was developed to estimate the lateral resistance per sleeper of a full-scale track panel. As mentioned earlier, the lateral sleeper resistance for 1/5-scale model tests is 1/125 of that of actual sleepers, and Eq. (3) is in agreement with this relationship. Eq. (3), therefore, corresponds to $R_{\text{single}}^{0.4\ \text{mm}}$, which is the lateral resistance at a horizontal displacement of 0.4 mm in the 1/5-scale model tests.

$$R_{\text{total}} \cong R_{\text{single}}^{0.4\ \text{mm}} \tag{4}$$

Considering the average ratio of $R_{\text{single}}^{0.4\ \text{mm}}$ to $R_{\text{single}}^{10\ \text{mm}}$, obtained from the model tests, $R_{\text{single}}^{10\ \text{mm}}$ can be approximately estimated using the following equation:

$$R_{\text{single}}^{10\ \text{mm}} = 1.30R_{\text{single}}^{0.4\ \text{mm}} \tag{5}$$

Using the guidelines in RTRI (2012), a, b, and c in Eq. (3) are determined to be 0.75, 29, and 1.8, respectively, and can be used to calculate $R_{\text{single}}^{0.4\ \text{mm}}$. Fig. 11 shows the relationship between lateral resistance $R_{\text{single}}^{0.4\ \text{mm}}$ and the lateral resistance estimated using Eq. (3). It should be noted that, in this study, S_{end} in Eq. (3) was evaluated for the winged sleepers using the cross sections of the wings, and not the cross sections of the sleeper ends. Otherwise, S_{end} of the winged sleepers with rectangular ends would be the same as that of the rectangular parallelepiped sleeper. This is not a reasonable approximation. It can be seen from the figure that Eq. (3) yields levels of lateral resistance which are comparable to those of the model tests. This suggests that Eq. (3) can be applied not only to conventional sleepers such as parallelepiped and 3H sleepers, but also to winged sleepers. However, as will be discussed

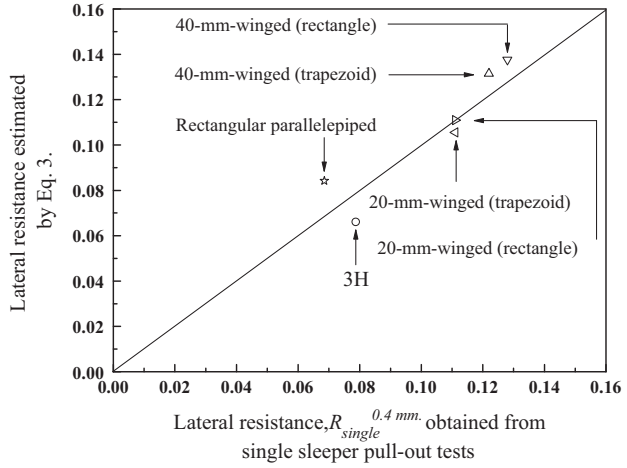

Fig. 11. Relationship between lateral resistance obtained from model test and that estimated by Eq. (3).

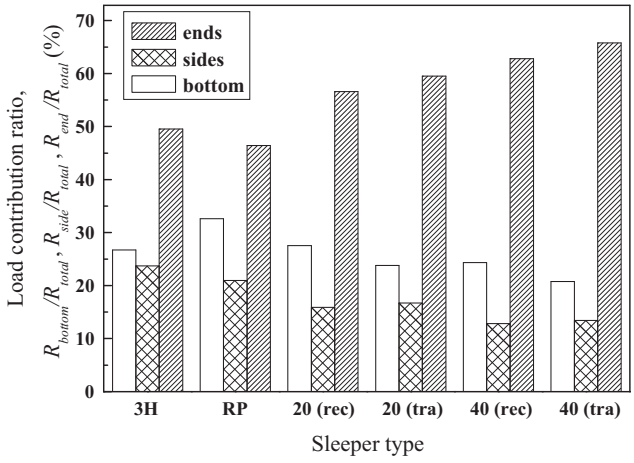

Fig. 12. Contributions of bottom resistance, side resistance, and end resistance to total resistance based on Eq. (3).

later, the lateral resistance obtained using Eq. (3) is not always close to that of track panel R_{panel}; it depends on the sleeper type.

The contributory effects of bottom resistance R_{bottom}, side resistance R_{side}, and end resistance R_{end} on the total resistance for each sleeper type, as estimated using Eq. (3), are shown in Fig. 12. In the figure, 3H, RP, 20(rec), 20(tra), 40(rec), and 40 (tra) represent the 3H sleeper, the rectangular parallelepiped sleeper, the 20-mm-winged sleepers with rectangular ends, the 20-mm-winged sleepers with trapezoidal ends, the 40-mm-winged sleepers with rectangular ends, and the 40-mm-winged sleepers with trapezoidal ends. It can be seen from the figure that the contributory effect of the end resistance of the 3H sleeper and that of the rectangular parallelepiped sleeper were both about 50%, whereas those of the 20-mm-winged sleepers were about 60% and those of the 40-mm-winged sleepers were about 65%. However, the contributory effects of the side resistance of the winged sleepers were smaller than those of the 3H and the rectangular parallelepiped sleepers. Similarly, the effects of the bottom resistance of the winged sleepers were relatively small, although their weights were greater.

4. Piled group effect on lateral resistance

4.1. Lateral resistance for track panel pullout tests using five sleepers

Track panel pullout tests using five sleepers were conducted on rectangular sleepers, 3H sleepers, 20-mm-winged sleepers with rectangular ends, and 20-mm-winged sleepers with trapezoidal ends. The results obtained from the tests are shown in Fig. 13. Fig. 13(a) shows the relationship between the horizontal load and the horizontal displacement for the sleepers. It can be seen from the figure that the relationship between the horizontal load and the horizontal displacement for the 20-mm-winged sleepers with rectangular ends is very similar to that for the 20-mm-winged sleepers with trapezoidal ends. The same relationship for the 3H sleeper is also similar to that for the rectangular parallelepiped sleepers. As mentioned in Section 3.1, these tendencies were also observed in the single-sleeper pullout tests (see Fig. 9(a)).

Fig. 13(b) shows the relationship between the horizontal displacement and the vertical displacement of the sleepers.

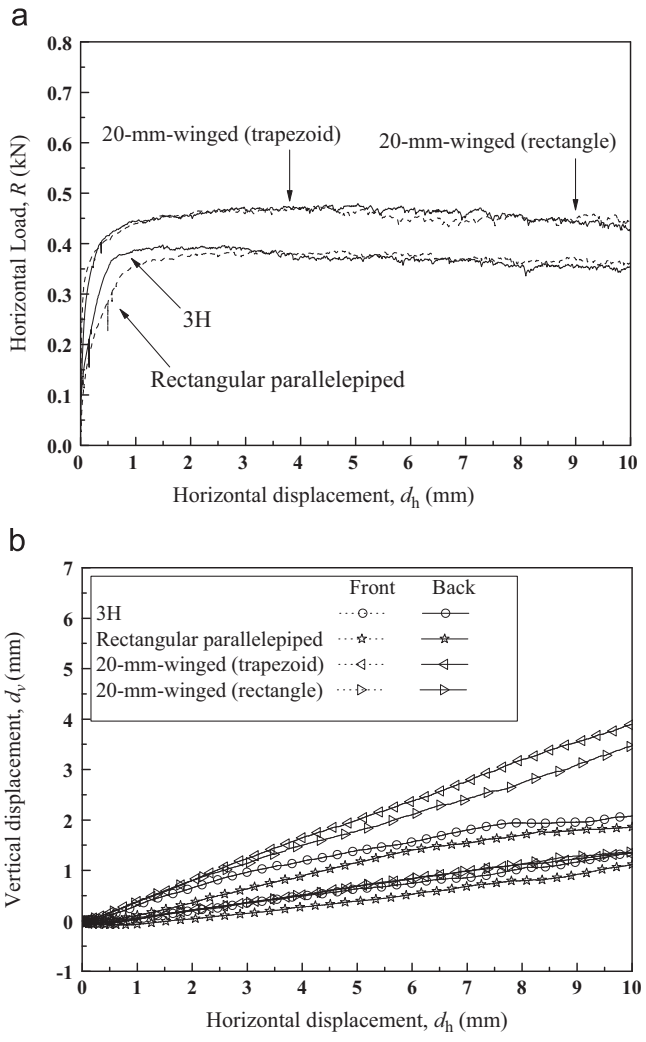

Fig. 13. Horizontal loads, vertical displacements, and horizontal displacements obtained from track panel loading tests. (a) Relationship between horizontal load and horizontal displacement and (b) relationship between vertical displacement and horizontal displacement.

The solid lines represent the vertical displacement measured at the sleeper end far from the loading jack (back side), whereas the dotted lines represent the vertical displacement measured at the sleeper end close to the loading jack (front side). The average values for both cases are shown. It can be seen from the figure that the sleepers moved upward, which is similar to the observations from Fig. 9(b). However, the upward movements observed in the track panel pullout tests were lower than those observed in the single-sleeper pullout tests. The reason for this was not properly understood during this study. However, as will be discussed later, it may be because the levels of lateral resistance per sleeper in the track panel pullout tests were lower than those in the single-sleeper pullout tests.

Fig. 14(a)–(d) shows the graphs of the horizontal load per sleeper against the displacement obtained from the single-sleeper pullout tests and track panel pullout tests. The horizontal loads obtained from the single-sleeper pullout tests were larger than those obtained from the track panel pullout tests for the five sleepers. Particularly, the levels of lateral resistance obtained from the single-sleeper pullout tests for the 20-mm-winged sleepers were quite a bit higher than those obtained from the track panel pullout tests. This issue will be discussed further.

Fig. 15 shows the lateral resistance obtained at a horizontal displacement of 0.4 mm in the single-sleeper pullout tests, $R_{\mathrm{single}}^{0.4\ \mathrm{mm}}$, and at a horizontal displacement of 10 mm in the track panel pullout tests, R_{panel}. It can be seen that $R_{\mathrm{single}}^{0.4\ \mathrm{mm}}$ is not close to R_{panel} for the 20-mm-winged sleepers. This suggests that, for full-scale winged sleepers, the lateral resistance obtained at a horizontal displacement of 2.0 mm in the single-sleeper pullout tests, $R_{\mathrm{single}}^{2.0\ \mathrm{mm}}$, should not be used to represent the lateral resistance in the track panel pullout tests.

In Fig. 16, the ratio of the lateral resistance obtained at a horizontal displacement of 10 mm in track panel pullout test R_{panel} to that obtained at the same displacement in single-sleeper pullout test $R_{\mathrm{single}}^{10\ \mathrm{mm}}$ is plotted against the sleeper width, which is normalized by the 116-mm sleeper spacing. Here, the width of the rectangular and the 3H sleepers is defined as the average width of the sleeper end, whereas the width of the winged sleepers is defined as the averaged width of the cross sections of the wings. The figure also shows the relationship fitted by the following equation:

$$(R_5/5)/R_{\mathrm{single}}^{10\ \mathrm{mm}} = 35(SW/SS)^2 - 76(SW/SS) + 100 \quad (0 \leqq SW/SS \leqq 1) \tag{6}$$

where R_5 is the lateral resistance obtained from the track panel pullout tests using five sleepers, SW is the sleeper width, and SS is the sleeper spacing.

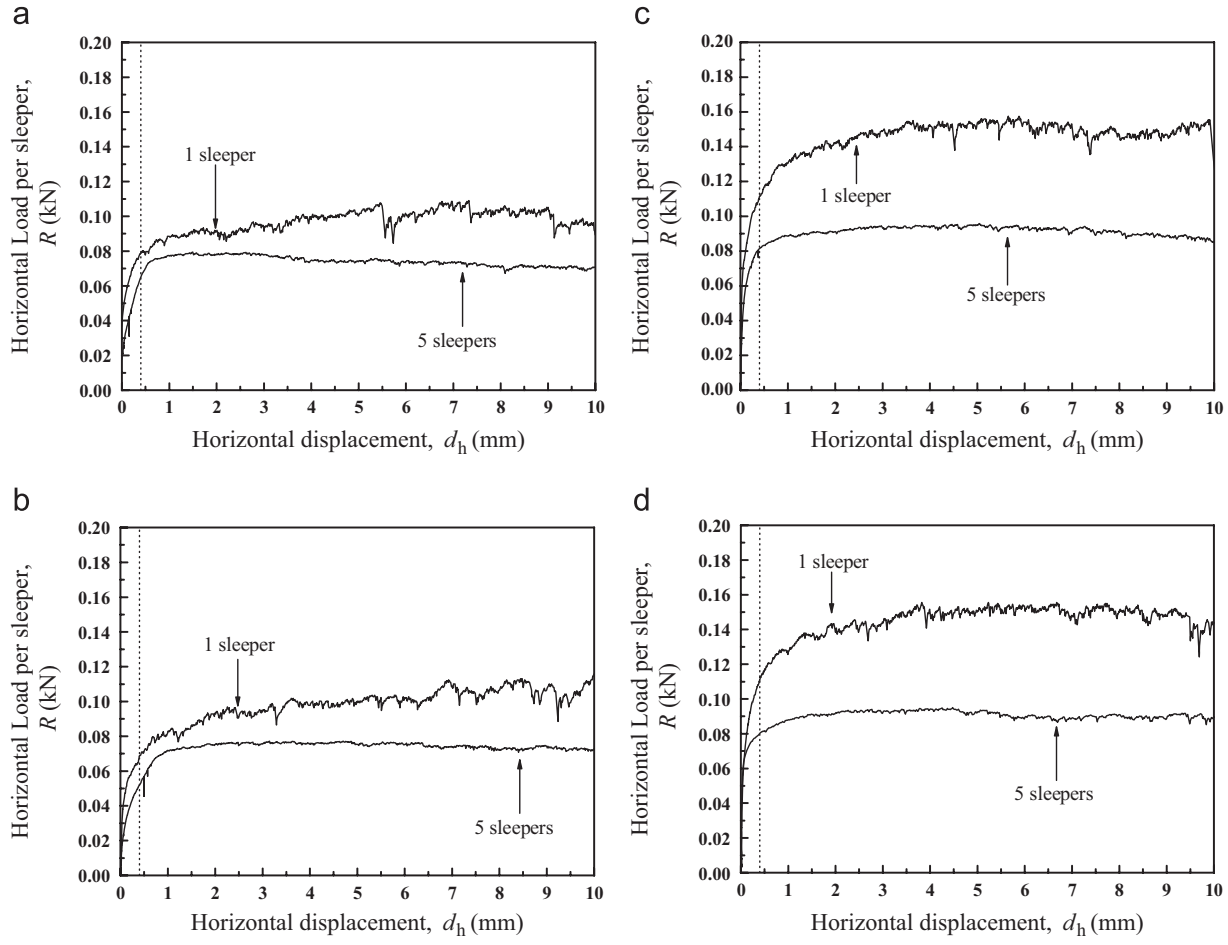

Fig. 14. Relationship between lateral resistance per sleeper and horizontal displacement obtained from single-sleeper pullout tests and track panel pullout tests. (a) 3H sleeper, (b) rectangular parallelepiped sleeper, (c) 20-mm-winged sleeper with trapezoidal ends and (d) 20-mm-winged sleeper with rectangular ends.

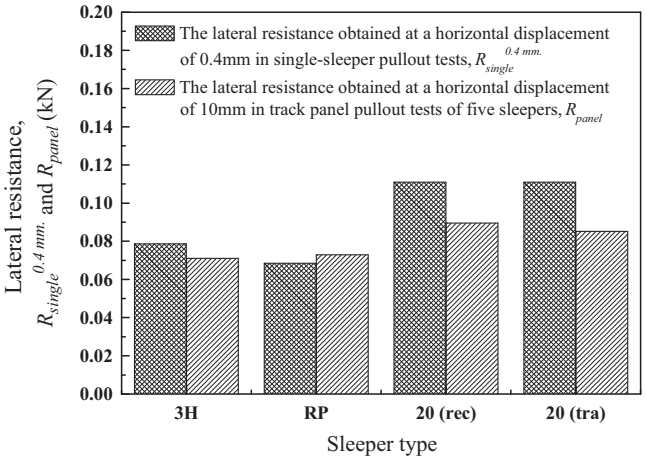

Fig. 15. Comparison of lateral resistance per sleeper obtained from track panel pullout tests and single-sleeper pullout tests.

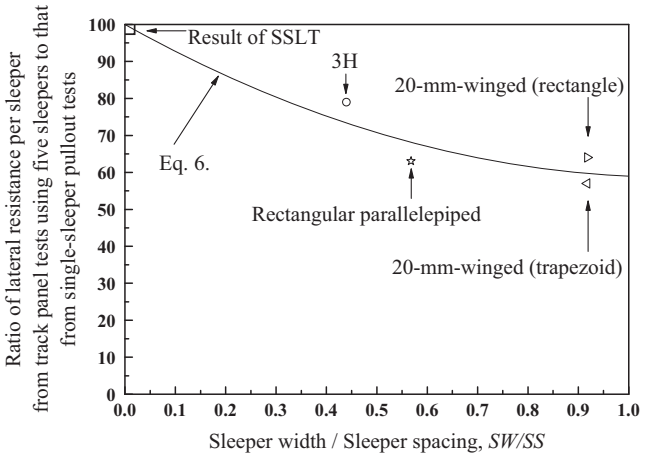

Fig. 16. Relationship between ratio of lateral resistance obtained from track panel pullout tests to that obtained from single-sleeper pullout tests, normalized by sleeper width.

As can be seen from the figure, the lateral resistance ratio, $R_{\mathrm{panel}}/R_{\mathrm{single}}^{10\ \mathrm{mm}}$, decreases significantly as the normalized sleeper width increases. This is due to the overlap of the ballast, which is affected by the adjacent sleepers. This phenomenon is similar to the so-called piled group effect. This will be confirmed in the next section.

4.2. Displacement of ballast during horizontal loading

In the single-sleeper pullout tests, a digital camera was set above the ballast to take consecutive images of the ballast and the sleepers during horizontal loading. PIV analyses were conducted on the images. Fig. 17 shows the displacements of the ballast obtained by the PIV analyses of the images taken at a horizontal displacement of 10 mm in the single-sleeper pullout tests of the 3H sleeper and the 20-mm-winged sleeper with trapezoidal ends. Fig. 17(a) shows the result for the 3H sleeper, and Fig. 17(b) shows that for the 20-mm-winged sleeper with trapezoidal ends. It can be seen from the figures

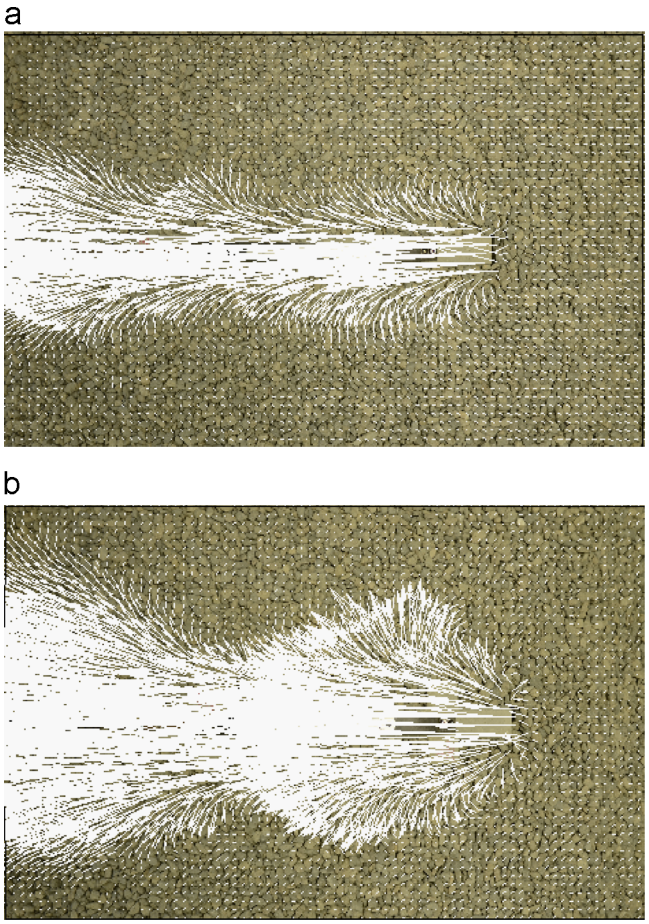

Fig. 17. Displacement of ballast analyzed by PIV at 10 mm horizontal displacement of sleeper in single-sleeper pullout tests. (a) 3H sleeper and (b) 20-mm-winged sleeper with trapezoidal ends.

that the displacement distribution for the 20-mm-winged sleeper with trapezoidal ends was wider than that for the 3H sleeper. This suggests that the piled group effect of the winged sleepers was more significant than that of the 3H sleeper in the track panel pullout tests.

5. Effect of number of sleepers on lateral resistance in track panel pullout tests

5.1. Effect of boundary and loading width

Track panel pullout tests using three or seven sleepers were also conducted on the 3H sleepers and the 20-mm-winged sleepers with trapezoidal ends. These were in addition to those conducted using five sleepers. The relationship between the horizontal load per sleeper and the horizontal displacement of the sleepers obtained from the track panel pullout tests are shown in Fig. 18. Fig. 18(a) shows the relationship for the 3H sleeper and Fig. 18(b) shows that for the 20–mm-winged sleeper with trapezoidal ends. The results for the single-sleeper pullout tests are also shown in the figures.

In both cases, the lateral resistance per sleeper in the track panel pullout tests decreased with an increasing number of sleepers. This was due to two factors. One was the effect of the

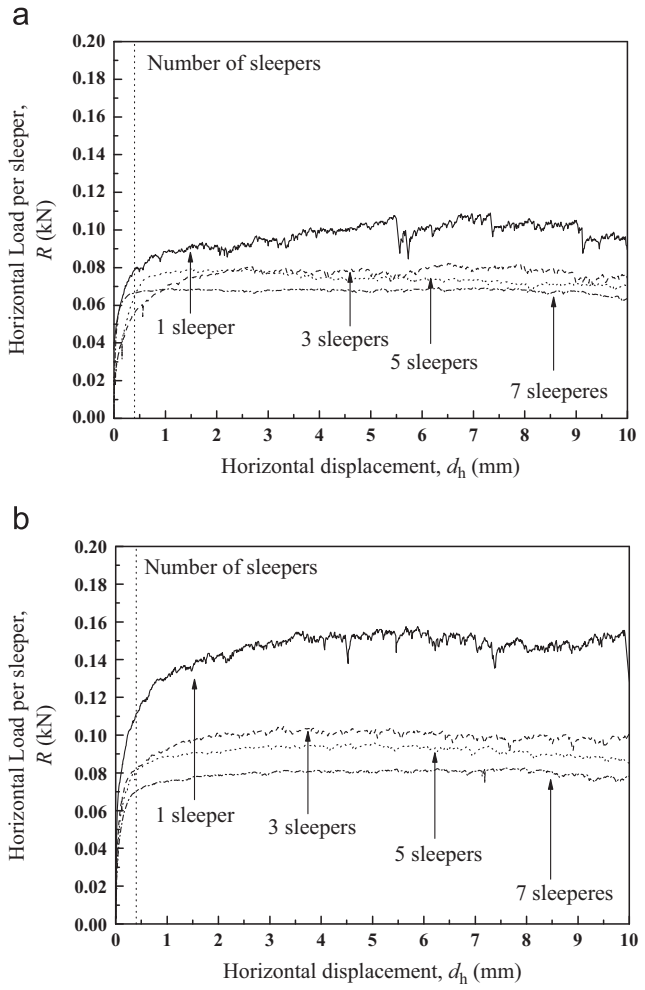

Fig. 18. Relationship between horizontal load and horizontal displacement of sleepers obtained from track panel loading tests using three, five, and seven sleepers. (a) 3H sleeper and (b) 20-mm-winged sleeper with trapezoidal end.

boundary shown in Fig. 19. As discussed in previous sections, there is a group effect (interaction effect) in the lateral resistance of the sleepers in the track panel pullout tests. The lateral resistance of the B-type sleepers in the figure should therefore be less than that of the A-type sleepers. This is because the piled group effect is much more dominant for the B-type sleepers. As the number of sleepers increased, the ratio of the number of B-type sleepers to the number of A-type sleepers increased, resulting in a reduction in the lateral resistance per sleeper in the track panel pullout tests.

The other factor was the effect of the distribution of the stress generated laterally from the sleeper ends to the ballast shoulders. As can be seen from Fig. 17, the ballast located along the lateral sides of the sleepers moved with the sleepers during horizontal loading. Similarly, in the track panel pullout tests, depending on the ratio of the sleeper width to the sleeper spacing, the ballast located along the lateral sides of the sleepers was entrapped and moved with the sleepers. Therefore, the apparent loading width, which includes the width of the entrapped ballast, increased with an increasing number of sleepers. The same observation was made in previously

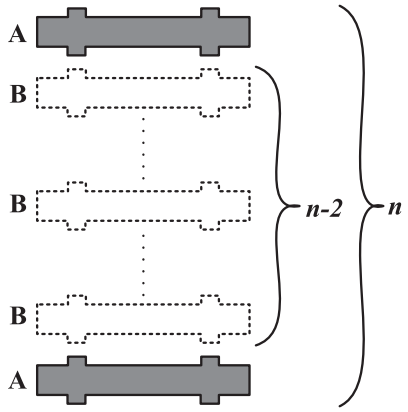

Fig. 19. Schematic of boundary effect in track panel loading tests.

reported results of vertical loading tests conducted on group piles (for example, Aoyama et al., 2013). The increased apparent loading width produced the wider stress distribution, indicating that stress can be generated in the ballast far from the sleeper ends. This increases the compression of the ballast and reduces the lateral resistance per sleeper.

5.2. Estimation of lateral resistance of sleepers in track panel tests using more than ten sleepers

The effect of the number of sleepers on the lateral resistance in the track panel pullout tests was discussed in the preceding section. Considering the actual buckling conditions, more than ten sleepers may be involved in the area where buckling occurs, depending on the temperature change, the rail stiffness, the sleeper lateral resistance, etc. (see Kerr, 1978; Lim et al., 2003). Therefore, in this section, we attempt to estimate the lateral resistance of the sleepers in the track panel pullout tests when more than ten sleepers are used. In the estimation, the piled group and the boundary effects observed in the track panel pullout tests are considered in the following manner.

First, the lateral resistance obtained from the single-sleeper pullout tests is denoted by R_{single}. Next, the total lateral resistance obtained from the track panel pullout tests, using n sleepers, is denoted by R_n ($n>2$). Actually, R_n is the sum of the lateral resistance of the B-type sleepers, R_B, and that of the A-type sleepers, R_A, as shown in Fig. 19. Therefore, R_n can be expressed as follows:

$$R_n = 2R_A + (n-2)R_B = 2\alpha R_{single} + (n-2)\beta R_{single} \quad (n>2) \tag{7}$$

here, α and β are the ratios of R_A to R_{single} and R_B to R_{single}, respectively. Therefore, to determine α and β, R_n must be estimated by conducting two track panel pullout tests using different numbers of sleepers. However, when we consider that the piled group effect of the lateral resistance of the A-type sleepers is induced by only one neighboring sleeper, whereas that of the B-type sleepers is induced by two neighboring sleepers, the following assumption is reasonable:

$$\alpha = (1+\beta)/2 \tag{8}$$

Introducing Eq. (8) into Eq. (7), we obtain

$$R_n = \{1+(n-1)\beta\}R_{\text{single}} \ (n>2) \tag{9}$$

From Eq. (9), we derive

$$R_n/n = \{1/n+(1-1/n)\beta\}R_{\text{single}} \ (n>2) \tag{10}$$

here, R_n/n is the lateral resistance per sleeper in the track panel pullout tests. Applying Eq. (10) to the results shown in Fig. 16, β can be obtained for each type of sleeper, and α can then be determined using Eq. (8).

Using the values for β thus obtained, the sleeper lateral resistance in the track panel tests for any arbitrary number of sleepers greater than two can be estimated using Eq. (10). It should be noted here that $R_{\text{single}}(n=1)$ can be estimated using the results of the single-sleeper pullout tests or the following equation, which can be derived from Eqs. 3–5:

$$R_n = R_{\text{single}} = 1.30\ (aW_{\text{sleeper}}+b\gamma_{\text{ballast}}S_{\text{end}}+c\gamma_{\text{ballast}}S_{\text{side}})\ (n=1) \tag{11}$$

The lateral resistance in the track panel tests using two sleepers, R_2, can then be estimated using the following equation:

$$R_n/n = \alpha R_{\text{single}} \ (n=2) \tag{12}$$

Fig. 20 shows the lateral resistance calculated using Eqs.10–12 for different numbers of sleepers. Fig. 21 shows the levels of lateral resistance obtained by the single-sleeper pullout tests, Eqs. (10), and (12), for different numbers of sleepers. A comparison of the experimental and the calculated results in the figures reveals that the proposed calculation method can be used for a reasonable evaluation of the lateral resistance for a wide range of sleeper numbers irrespective of the sleeper type. The calculation results for both cases also suggest that the lateral resistance per sleeper stabilizes at a given value with an increasing number of sleepers.

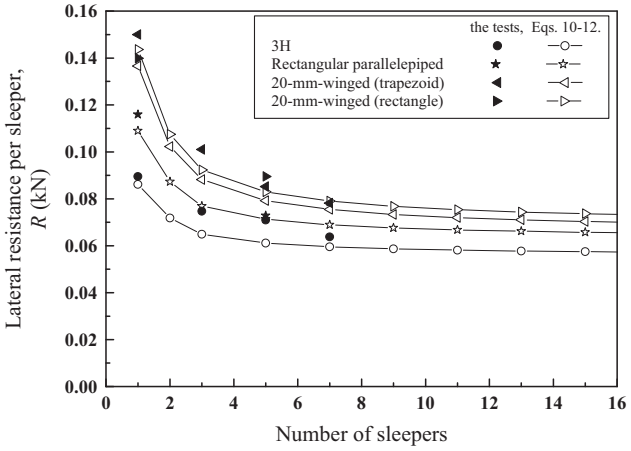

Fig. 20. Relationship between lateral resistance per sleeper and sleeper number in pullout tests. (R_{single} obtained by equations).

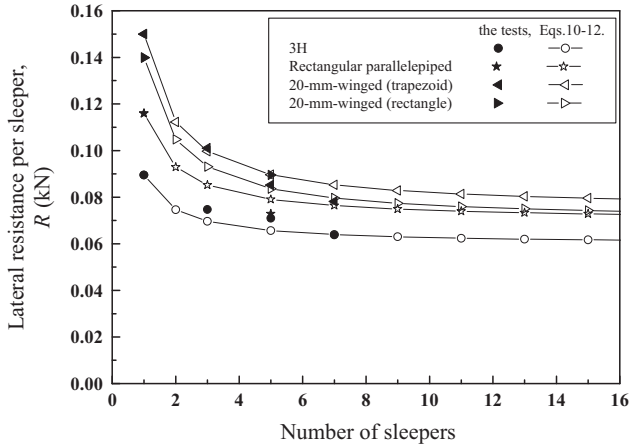

Fig. 21. Relationship between lateral resistance per sleeper and sleeper number in pullout tests. (R_{single} obtained from tests).

6. Conclusions

In this study, a series of tests was conducted on 1/5-scale models to evaluate the lateral resistance of the sleepers of ballasted tracks. Single-sleeper pullout tests and track panel pullout tests were conducted on several types of concrete sleepers to investigate the effects of the sleeper shape, the sleeper spacing, and the number of sleepers on the lateral resistance. From the results, we draw the following conclusions:

(1) The side frictional resistance, the end resistance, and the bottom resistance significantly affect the total lateral resistance of the sleepers. The prediction method proposed in RTRI (2012) is not only valid for conventional sleepers, but also for winged sleepers.
(2) However, the idea that the lateral resistance measured at a horizontal displacement of 2.0 mm in full-scale (or 0.4 mm in 1/5-scale) single-sleeper pullout tests corresponds to that in track panel pullout tests is only valid under limited conditions. This is because of the piled group effect in track panel pullout tests, which affects the lateral resistance. As the degree of the piled group effect is controlled by the ratio of sleeper width to sleeper spacing, a significant reduction in lateral resistance may be observed in track panel pullout tests depending on the sleeper type.
(3) The lateral resistance per sleeper in track panel pullout tests decreases with an increasing number of sleepers. This is due to the boundary conditions and the loading width. The group effect on the sleepers close to the free ends of a rigid frame is insignificant compared to that on the sleepers far from the free ends, and the effect on those close to the free ends decreases with an increasing number of sleepers. Also, the ballast along the lateral sides of the sleepers is entrapped and moves with the sleepers. The consequent apparent increase in loading width broadens the stress distribution, and thereby, increases the compression of the ballast, resulting in a reduction in the lateral resistance per sleeper.

(4) Based on the results of the model tests, we have proposed a new calculation method for estimating the lateral resistance of sleepers in track panel tests for a wide range in numbers of sleepers. This estimation method considers the piled group and the boundary effects observed in the track panel pullout tests. A comparison of the experimental and the calculation results reveals that the proposed calculation method can be used to reasonably evaluate the lateral resistance of all types of sleepers. The calculation results also suggest that the lateral resistance per sleeper stabilizes at a given value with an increasing number of sleepers.

Acknowledgment

We acknowledge the assistance of Mr. Shigekuni of the Tokyo Metropolitan Government, a former graduate student of Yokohama National University, in the preparation for the model tests.

References

Aoyama, S., Bangan, L., Renzo, A. A., Danardi, L., Goto, S., Towhata, I., 2013. Application of advanced sensors to model tests on bearing mechanism of group pile. In: Yao, Y., Watabe, Y., Hu, w., (Eds.), New Advances in Geotechnical Engineering, pp. 65–74.

Arbabi, F., Khalighi, M., 2011. Stability of railroad tracks under the effects of temperature change and earthquake. J. Seismol. Earthq. Eng. 12 (3), 119–129.

Asanuma, K., Tomita, K., Sogabe, M., 2012. Study on temperature of ballasted track by elasto-plastic and finite displacement analyses. J. Jpn. Soc. Civ. Eng. Ser. A2 (Appl. Mech.) 68 (1), 78–91 (in Japanese).

Bao, Y., Barenberg, E.J., 1997. Three-dimensional nonlinear stability analysis of tangent continuous welded rail track under temperature and mechanical loads. Transp. Res. Rec.: J. Transp. Res. Board 1584, 31–40.

Dahlberg, T., 2001. Some railroad settlement models – a critical review. Proc. Inst. Mech. Eng. Part F: J. Rail Rapid Transit 215, 289–299.

Indraratna, B., 2011. Advanced Rail Geotechnology Ballasted Track. CRC Press, pp. 154–162.

Ishikawa, T., Namura, A., 1995. Cyclic deformation characteristics of railroad ballast in full-scale tests. J. Japanese Soc. Civ. Eng. No. 512, 47–59 (in Japanese).

Kabo, E., 2006. A numerical study of the lateral ballast resistance in railway tracks. Proc. Inst. Mech. Eng. Part F: J. Rail Rapid Transit 220, 425–433.

Kerr, A.D., 1978. Analysis of thermal track buckling in the lateral plane. Acta Mech 30 (1), 17–50.

Kerr, A.D., 2004. Fundamentals of Railway Track Engineering. Simmons-Boardman Publishing Corporation, pp. 1–391.

Kusuda, M., Yamaguchi, Y., Momoya, Y., Ito, I. 2012, Study on roadbed lateral resistance in ballasted tracks from model tests. In: Proceedings of the 67th Annual Meeting of Japan Society for Civil Engineers. VI-528, CD-ROM (in Japanese).

Le Pen, L.M., Powrie, W., 2012. Contribution of base, crib, and shoulder ballast to the lateral sliding resistance of railway track: a geotechnical perspective. Proc. Inst. Mech. Eng. Part F, J. Rail Rapid Transit 225 (2), 113–128.

Lichtberger, B., 2007. The lateral resistance of the track. Eur. Railw. Rev. 13 (3–4), 68–71.

Lim, N.H., Park, N.H., Kan, Y.J., 2003. Stability of continuous welded rail track. Comput. Struct. 81, 2219–2236.

Momoya, Y., Sekine, E., Tatsuoka, F., 2005. Deformation characteristics of railway roadbed and subgrade under moving-wheel load. Soils Found. 45 (4), 99–118.

Nakamura, T., Sekine, E., Shirae, Y., 2010. Evaluation of seismic performance in ballasted tracks from large-scale shaking table tests. Railw. Tech. Res. Rep. 24 (12) (in Japanese).

Namura, A., Kohata, Y., Miura, S., 2005. Experimental study on effect of loading condition and sleeper size on deformation properties of railway ballast. J. Japanese Soc. Civ. Eng. IV-66 (779), 53–68 (in Japanese).

Railway Technical Research Institute, 2012. Design standards for railway structures and commentary. Track Struct, 431 (in Japanese).

Takatani, H., Sato, Y., Suzuki, S., 1987. Temperature Rising Test of Turnout. Railway Technical Research Pre-report. No. A-87-214, pp. 1–51 (in Japanese).

Xavier, P., 2012. Reliability and Safety in Railway. InTech. Chapter 3.

Zakeri, J.A., Sadeghi, J., 2007. Field investigation on load distribution and deflections of railway track sleepers. J. Mech. Sci. Technol. 21 (12), 1948–1956.

Zakeri, J.A., Mirfattahi, B., Fakhari, M., 2012. Lateral resistance of railway track with frictional sleepers. Proc. Inst. Civ. Eng. – Transp. J. 165 (2), 151–155.